

Mechanistic Studies on Oxidative Addition of Aryl Halides and Triflates to Pd(BINAP)₂ and Structural Characterization of the Product from Aryl Triflate Addition in the Presence of Amine

Luis M. Alcazar-Roman and John F. Hartwig*

Department of Chemistry, Yale University, P.O. Box 208107,
New Haven, Connecticut 06520-8107

Received September 10, 2001

Kinetic studies of the oxidative addition of phenyl iodide and phenyl triflate to Pd(BINAP)₂ (**1**) are reported. The products of the oxidative addition of phenyl trifluoromethanesulfonate to **1** in the presence of the primary amines *n*-octylamine and isoamylamine are the cationic aryl palladium(II) complexes [(BINAP)Pd(Ph)(H₂NR)]OTf (**2a,b**), and the product of the oxidative addition of phenyl iodide to **1** is the phenylpalladium iodide {(BINAP)Pd(Ph)I} (**3**). Structural characterization of the rare, stable σ -aryl Pd(II) triflate complex (**2b**), in this case coordinated by isoamylamine, is reported. Initial mechanistic studies focused on measuring the rates of reactions containing concentrations of aryl electrophile ranging from 8.94×10^{-7} to 0.2 M. Under these conditions, the oxidative addition of PhOTf and PhI to **1** was inverse first-order in added BINAP ligand when the concentration of ArX was low. The oxidative addition reaction was first-order in ArX when the concentration of ArX was low and was zero order in ArX when the concentration of ArX was high. At these high concentrations, the reaction rate depended solely on the rate for dissociation of BINAP from **1**. However, additional experiments using concentrations of aryl iodide and aryl bromide up to 4.0 M led to a measurable increase in observed rate constants and detection of a second concurrent reaction mechanism. This effect was not observed with phenyl triflate. The relevance of this phenomenon to catalytic coupling and oxidative addition of aryl bromides is discussed. Reactions of triflate complex **2a** with several bases to form *N*-octylaniline are also reported.

Introduction

The oxidative addition of aryl halides and sulfonates to Pd(0) is a fundamental organometallic transformation.^{1,2} It is the first step in the palladium-catalyzed coupling of organic electrophiles with a variety of carbon nucleophiles (such as carbonyl enolates,^{3–6} organomagnesium,^{7–13} boron,^{14–24} and tin^{25,26} reagents) and heteroatom nucleophiles (thiols,^{27–30} amines,^{31–35}

imines,^{36–40} azoles,³⁹ alcohols,^{41–46} phenols^{47,48}), as well as in the palladium-catalyzed arylation of olefins

(1) Collman, J. P.; Hegedus, L. S.; Norton, J. R.; Finke, R. G. *Principles and Applications of Organotransition Metal Chemistry*, 2nd ed.; Wiley-Interscience: New York, 1987; pp 322–333.

(2) Stille, J. K.; Lau, K. S. Y. *Acc. Chem. Res.* **1977**, *10*, 4–442.

(3) Shaughnessy, K. H.; Hamann, B. C.; Hartwig, J. F. *J. Org. Chem.* **1998**, *63*, 6546–6553.

(4) Hamann, B. C.; Hartwig, J. F. *J. Am. Chem. Soc.* **1997**, *119*, 12382.

(5) Palucki, M.; Buchwald, S. L. *J. Am. Chem. Soc.* **1997**, *119*, 11108–11109.

(6) Ahman, J.; Wolfe, J. P.; Troutman, M. V.; Palucki, M.; Buchwald, S. L. *J. Am. Chem. Soc.* **1998**, *120*, 1918–1919.

(7) Rehm, J. D. D.; Ziemer, B.; Sziemies, G. *Eur. J. Org. Chem.* **1999**, *2079*, 9–2085.

(8) Bumagin, N. A.; Luzikova, E. V.; Beletskaya, I. P. *Zh. Org. Khim.* **1995**, *31*, 1663–1666.

(9) Bumagin, N. A.; Sokolova, A. A.; Beletskaya, I. P.; Wolz, G. *Zh. Org. Khim.* **1993**, *29*, 162–164.

(10) Bumagin, N. A.; Andryukhova, N. P.; Beletskaya, I. P. *Dokl. Akad. Nauk SSSR* **1987**, *297*, 1126–1129.

(11) Hayashi, T.; Konishi, M.; Kumada, M. *Tetrahedron Lett.* **1979**, *21*, 1871–1874.

(12) Hayashi, T.; Konishi, M.; Kobori, Y.; Kumada, M.; Higuchi, T.; Hirotsu, K. *J. Am. Chem. Soc.* **1984**, *106*, 158–163.

(13) Kranenburg, M.; Kamer, P. C. J.; Van Leeuwen, P. W. N. M. *Eur. J. Inorg. Chem.* **1998**, 155–157.

(14) Nicolau, K. C.; Li, H.; Boddy, C. N. C.; Ramanjulu, J. M.; Yue, T.; Natarajan, S.; Chu, X.; Brase, S.; Rubsam, F. *Chem.-Eur. J.* **1999**, *5*, 2584–2601.

(15) Uozumi, Y.; Suzuki, N.; Ogiwara, A.; Hayashi, T. *Tetrahedron* **1994**, *50*, 4293–4302.

(16) Vanier, C.; Wagner, A.; Mioskowski, C. *Tetrahedron Lett.* **1999**, *40*, 4335–4338.

(17) Firooznia, F.; Gude, C.; Chan, K.; Marcopulos, N.; Satoh, Y. *Tetrahedron Lett.* **1999**, *40*, 213–216.

(18) Gemma, E.; Lopez-Sanchez, M. A.; Martinez, M. E.; Plumet, J. *Tetrahedron* **1998**, *54*, 197–212.

(19) Kowitz, C.; Wegner, G. *Tetrahedron* **1997**, *53*, 15553–15574.

(20) Matos, K.; Soderquist, J. A. *J. Org. Chem.* **1998**, *63*, 461–470.

(21) Setayesh, S.; Bunz, U. H. F. *Organometallics* **1997**, *15*, 55470–5472.

(22) Fuerstner, A.; Seider, G. *Tetrahedron* **1995**, *54*, 11165–11176.

(23) Ohe, T.; Miyaura, N.; Suzuki, A. *J. Org. Chem.* **1993**, *58*, 2201–2208.

(24) Ishiyama, T.; Kizaki, H.; Hayashi, T.; Suzuki, A.; Miyaura, N. *J. Org. Chem.* **1998**, *63*, 4726–4731.

(25) Newhouse, B. J.; Meyers, A. I.; Sirisoma, N. S.; Braun, M. P.; Johnson, C. R. *Synlett* **1993**, 573–574.

(26) Attwood, M. R.; Raynham, T. M.; Smyth, D. G.; Stephenson, G. R. *Tetrahedron Lett.* **1996**, *37*, 2731–2734.

(27) Hartwig, J. F. *Acc. Chem. Res.* **1998**, *31*, 852–860.

(28) Mann, G.; Baranano, D.; Hartwig, J. F.; Rheingold, A. L.; Guzei, I. A. *J. Am. Chem. Soc.* **1998**, *120*, 9205–9219.

(29) Barañano, D.; Hartwig, J. F. *J. Am. Chem. Soc.* **1995**, *117*, 2937–2938.

(30) Zheng, N.; McWilliams, J. C.; Fleitz, F. J.; Armstrong, J. D.; Volante, R. P. *J. Org. Chem.* **1998**, *63*, 9606–9607.

(Heck reaction).^{49–68} Often, palladium complexes ligated by chelating bisphosphines are efficient catalysts for these reactions. The use of palladium complexes of chelating phosphines, such as DPPF,⁶⁹ has improved reaction selectivity relative to that of catalysts ligated by monodentate phosphines such as PPh₃ and P(*o*-Tol)₃.^{7–13,16–26,31,32,65–68,70–92} Likewise, BINAP⁶⁹ has been used as a ligand to confer enantioselectivity in the product of a coupling reaction or simply as an effective and convenient supporting

ligand.^{3,5,6,14,15,33,35,37,38,49–64,93–98} Oxidative addition initiates the catalytic cycle in many cross-coupling processes, and it can even be the turnover-limiting step.^{99,100} It is, therefore, surprising that few studies have addressed the mechanism of oxidative addition of aryl halides or sulfonates to Pd(0) ligated by chelating phosphines,^{101–103} while many reports document mechanistic features of the oxidative addition of aryl halides and sulfonates to Pd(PPh₃)₄.^{104–109}

- (31) Driver, M. S.; Hartwig, J. F. *J. Am. Chem. Soc.* **1997**, *119*, 8232–8245.
- (32) Driver, M. S.; Hartwig, J. F. *J. Am. Chem. Soc.* **1996**, *118*, 7217–7218.
- (33) Wagaw, S.; Rennels, R. A.; Buchwald, S. L. *J. Am. Chem. Soc.* **1997**, *119*, 8451–8458.
- (34) Singer, R. A.; Buchwald, S. L. *Tetrahedron Lett.* **1999**, *40*, 1095–1098.
- (35) Wolfe, J. P.; Buchwald, S. L. *J. Org. Chem.* **2000**, *65*, 1144–1157.
- (36) Bolm, C.; Hildebrand, J. P. *Tetrahedron Lett.* **1998**, *39*, 5731–5734.
- (37) Bolm, C.; Hildebrand, J. P.; Rudolph, J. *Synthesis* **2000**, 911–913.
- (38) Bolm, C.; Hildebrand, J. P. *J. Org. Chem.* **2000**, *65*, 169–175.
- (39) Mann, G.; Hartwig, J. F.; Driver, M. S.; Fernandez-Rivas, C. *J. Am. Chem. Soc.* **1998**, *120*, 827–828.
- (40) Wolfe, J. P.; Åhman, J.; Sadighi, J. P.; Singer, R. A.; Buchwald, S. L. *Tetrahedron Lett.* **1997**, *38*, 6367–6370.
- (41) Widenhofer, R. A.; Zhong, H. A.; Buchwald, S. L. *J. Am. Chem. Soc.* **1997**, *119*, 6787–6795.
- (42) Widenhofer, R. A.; Buchwald, S. L. *J. Am. Chem. Soc.* **1998**, *120*, 6504–6511.
- (43) Palucki, M.; Wolfe, J. P.; Buchwald, S. L. *J. Am. Chem. Soc.* **1996**, *118*, 10333–10334.
- (44) Mann, G.; Hartwig, J. F. *J. Am. Chem. Soc.* **1996**, *118*, 13109–13110.
- (45) Mann, G.; Hartwig, J. F. *J. Org. Chem.* **1997**, *62*, 5413–5418.
- (46) Palucki, M.; Wolfe, J. P.; Buchwald, S. L. *J. Am. Chem. Soc.* **1997**, *119*, 3395–3396.
- (47) Mann, G.; Hartwig, J. F. *Tetrahedron Lett.* **1997**, *38*, 8005–8008.
- (48) Aranyos, A.; Old, D. W.; Kiyomori, A.; Wolfe, J. P.; Sadighi, J. P.; Buchwald, S. L. *J. Am. Chem. Soc.* **1999**, *121*, 4369–4378.
- (49) Sato, Y.; Sodeoka, M.; Shibasaki, M. *J. Org. Chem.* **1989**, *54*, 4738–4739.
- (50) Ashimori, A.; Bachand, B.; Calter, M. A.; Govek, S. P.; Overman, L. E.; Poon, D. J. *J. Am. Chem. Soc.* **1998**, *120*, 6488–6499.
- (51) Ashimori, A.; Bachand, B.; Overman, L. E.; Poon, D. J. *J. Am. Chem. Soc.* **1998**, *120*, 6477–6487.
- (52) Oshima, T.; Kegechika, K.; Adachi, M.; Sodeoka, M.; Shibasaki, M. *J. Am. Chem. Soc.* **1996**, *118*, 7108–7116.
- (53) Tietze, L. F.; Raschke, T. *Synlett* **1995**, 597–598.
- (54) Kurihara, Y.; Sodeoka, M.; Shibasaki, M. *Chem. Pharm. Bull.* **1994**, *42*, 2357–2359.
- (55) Kondo, K.; Sodeoka, M.; Mori, M.; Shibasaki, M. *Tetrahedron Lett.* **1993**, *34*, 4219–4222.
- (56) Takemoto, T.; Sodeoka, M.; Sasai, H.; Shibasaki, M. *J. Am. Chem. Soc.* **1993**, *115*, 8477–8478.
- (57) Sato, Y.; Sodeoka, M.; Shibasaki, M. *Chem. Lett.* **1990**, 1953–1954.
- (58) Ashimori, A.; Overman, L. E. *J. Org. Chem.* **1992**, *57*, 4571–4572.
- (59) Yoshida, M.; Sugimoto, K.; Ihara, M. *Tetrahedron Lett.* **2000**, *41*, 5089–5092.
- (60) Hayashi, T.; Tang, J.; Kato, K. *Org. Lett.* **1999**, *1*, 1487–1489.
- (61) Tietze, L. F.; Thede, K. *J. Chem. Soc., Chem. Commun.* **1999**, 1811–1812.
- (62) Sonesson, C.; Larhed, M.; Nyqvist, C.; Hallberg, A. *J. Org. Chem.* **1996**, *61*, 4756–4763.
- (63) Ozawa, F.; Hayashi, T. *J. Organomet. Chem.* **1992**, *428*, 267–277.
- (64) Ozawa, F.; Kubo, A.; Hayashi, T. *Tetrahedron Lett.* **1992**, *33*, 1485–1488.
- (65) Larhed, M.; Andersson, C. M.; Hallberg, A. *Tetrahedron* **1994**, *50*, 285–304.
- (66) Cabri, W.; Candiani, I.; Bedeschi, A.; Penco, S.; Santi, R. *J. Org. Chem.* **1992**, *57*, 1481–1486.
- (67) Cabri, W.; Candiani, I.; DeBernardinis, S.; Francalanci, F.; Penco, S.; Santo, R. *J. Org. Chem.* **1991**, *56*, 5796–5800.
- (68) Olofsson, K.; Larhed, M.; Hallberg, A. *J. Org. Chem.* **1998**, *63*, 5076–5079.
- (69) DPPF = 1,1'-bis(diphenylphosphino)ferrocene; BINAP = 2,2'-bis(diphenylphosphino)-1,1'-binaphthyl.
- (70) Arcadi, A.; Cacchi, S.; Marinelli, F.; Pace, P.; Sanzi, G. *Synlett* **1995**, 823–824.
- (71) Bumagin, N. A.; Angryukhova, N. P.; Beletskaya, I. P. *Metalloorg. Khim.* **1989**, *2*, 893–897.
- (72) Bumagin, N. A.; Sikolova, A. F.; Beletskaya, I. P. *Izv. Akad. Nauk, Ser. Khim.* **1993**, 2009–2010.
- (73) Bumagin, N. A.; Safarov, F. S.; Beletskaya, I. P. *Dokl. Akad. Nauk* **1993**, *332*, 48–49.
- (74) Cabri, W.; Candiani, I.; Bedeschi, A.; Santi, R. *J. Org. Chem.* **1992**, *57*, 3558–3563.
- (75) Cacchi, S.; Ciattini, P. G.; Morera, E.; Ortar, G. *Tetrahedron Lett.* **1986**, *27*, 3931–3934.
- (76) Cacchi, S.; Ciattini, P. G.; Morera, E.; Ortar, G. *Tetrahedron Lett.* **1986**, *24*, 5541–5544.
- (77) Cacchi, S.; Lupi, A. *Tetrahedron Lett.* **1992**, *33*, 3939–3942.
- (78) Carfagna, C.; Musco, A.; Sallèse, G.; Santi, R.; Fiorani, T. *J. Org. Chem.* **1991**, *56*, 216–263.
- (79) Ciattini, P. G.; Morera, E.; Ortar, G. *Tetrahedron Lett.* **1995**, *36*, 4133–4136.
- (80) Coudret, C.; Mazenc, V. *Tetrahedron Lett.* **1997**, *38*, 5293–5296.
- (81) Flandanese, V.; Miccoli, G.; Naso, F.; Ronzini, L. *J. Organomet. Chem.* **1986**, *312*, 343–348.
- (82) Fuerstner, A.; Seider, G. *Synlett* **1998**, 161–162.
- (83) Gaumon, A.; Brown, J. M.; Hursthouse, M. B.; Coles, S. J. *J. Chem. Soc., Chem. Commun.* **1999**, 63–64.
- (84) Ishiyama, T.; Itoh, Y.; Kiatano, T.; Miyaura, N. *Tetrahedron Lett.* **1997**, *38*, 3447–3450.
- (85) Messner, M.; Kozhushkov, S. I.; De Meijere, A. *Eur. J. Org. Chem.* **2000**, 1137–1155.
- (86) Molander, G. A.; Ito, K. *Org. Lett.* **2001**, *3*, 393–396.
- (87) Murata, M.; Oyama, T.; Watanabe, S.; Masuda, Y. *J. Org. Chem.* **2000**, *65*, 164–168.
- (88) Piber, M.; Jensen, A. E.; Rottlaender, M.; Knochel, P. *Org. Lett.* **1999**, *1*, 1323–1326.
- (89) Rottaender, M.; Palmer, N.; Knochel, P. *Synlett* **1996**, 573–575.
- (90) Rozenberg, V. I.; Sergeeva, E. V.; Kharitonov, V. G.; Vorontsova, N. V.; Vorontsova, E. V.; Mikul'shina, V. V. *Izv. Akad. Nauk, Ser. Khim.* **1994**, 1081–1085.
- (91) Ruhland, B.; Bombrun, A.; Gallop, M. A. *J. Org. Chem.* **1997**, *62*, 7820–7826.
- (92) Takagi, K.; Iwachido, T.; Hayama, N. *Chem. Lett.* **1987**, 839–840.
- (93) Olivera, R.; San Martin, R.; Dominguez, E. *Tetrahedron Lett.* **2000**, *41*, 4357–4360.
- (94) Ozawa, F.; Kubo, A.; Matsumoto, Y.; Hayashi, T. *Organometallics* **1993**, *12*, 4188–4196.
- (95) Sedeoka, M.; Tokunoh, R.; Miyazaki, F.; Hagiwara, E.; Shibasaki, M. *Synlett* **1997**, 463–466.
- (96) Vyskocil, S.; Jaracz, S.; Smrcina, M.; Sticha, M.; Hanus, V.; Polasek, M.; Kocovsky, P. *J. Org. Chem.* **1998**, *63*, 7727–7737.
- (97) Vyskocil, S.; Smrcina, M.; Kocovsky, P. *Tetrahedron Lett.* **1998**, *39*, 9289–9292.
- (98) Wolfe, J. P.; Wagaw, S.; Buchwald, S. L. *J. Am. Chem. Soc.* **1996**, *118*, 7215–7216.
- (99) Alcazar-Roman, L. M.; Hartwig, J. F.; Rheingold, A. L.; Liable-Sands, L. M.; Guzei, I. A. *J. Am. Chem. Soc.* **2000**, *122*, 4618–4630.
- (100) Littke, A. F.; Dai, C. Y.; Fu, G. C. *J. Am. Chem. Soc.* **2000**, *122*, 4020–4028.
- (101) Amatore, C.; Broeker, G.; Jutand, A.; Khalil, F. *J. Am. Chem. Soc.* **1997**, *119*, 5176–5185.
- (102) Jutand, A.; Hii, K. K. M.; Thornton-Pett, M.; Brown, J. M. *Organometallics* **1999**, *18*, 5367–5374.
- (103) Portnoy, M.; Milstein, D. *Organometallics* **1993**, *12*, 1665–1673.
- (104) Amatore, C.; Azzabi, M.; Jutand, A. *J. Am. Chem. Soc.* **1991**, *113*, 1670–1677.
- (105) Amatore, C.; Jutand, A.; M'Barki, M. A. *Organometallics* **1992**, *11*, 3009–3013.
- (106) Amatore, C.; Jutand, A.; Suarez, A. *J. Am. Chem. Soc.* **1993**, *115*, 9531–9541.
- (107) Amatore, C.; Jutand, A.; Meyer, G. *Inorg. Chim. Acta* **1998**, *273*, 76–84.
- (108) Amatore, C.; Jutand, A. *J. Organomet. Chem.* **1999**, *573*, 254–278.

The reactivity of aryl halide electrophiles toward Pd(0) is typically $\text{ArI} > \text{ArBr} \approx \text{ArOTf} \gg \text{ArCl}$.¹ The difference in the reactivity of ArX has been linked to the difference in C–X bond strengths, a factor that would affect the rate of oxidative addition when the rate-limiting step of this process is C–X bond scission. However, we have shown recently that ligand dissociation and not C–X bond cleavage is the rate-limiting step of aryl bromide oxidative addition to Pd(0) when the concentration of aryl bromide is high. Therefore, the turnover-limiting step of a catalytic cycle can be ligand dissociation.⁹⁹ In these cases, the reactivity of the aryl halide does not control the rate of oxidative addition.

The products from oxidative addition of aryl triflates are generally unstable, and few have been isolated in pure form.^{109–111} Jutand and Mosleh reported that the product from oxidative addition of phenyl triflate to Pd(PPh_3)₄ is a cationic (σ -aryl)palladium complex that is stabilized by coordination of the DMF solvent used in these reactions.¹⁰⁹ Most aryl triflate complexes of palladium ligated by chelating phosphines are also less stable than aryl halide complexes.¹¹² Brown reported the in situ generation and characterization of [(BINAP)Pd(Ph)(THF)]OTf at -78°C .¹¹¹ Jutand has observed clean reactions of aryl triflates with (DPPF)Pd(η^2 -methylacrylate), but only in the presence of coordinating anions, such as iodide and acetate.¹⁰²

The absence of these addition products has hampered detailed studies on the oxidative addition of aryl triflates to Pd(0). Studies with platinum model complexes have been reported, but these studies do not address directly the relative rates for different elementary reactions in the multistep addition process with palladium.¹¹³ Jutand and Mosleh described the mechanism for oxidative addition of aryl triflates to Pd(PPh_3)₄¹⁰⁹ and showed that a mechanism similar to that for the previously studied oxidative addition of aryl iodides to Pd(PPh_3)₄ was followed.¹⁰⁶ Jutand and Brown reported the mechanism of oxidative addition of aryl triflates to the zerovalent (DPPF)Pd(η^2 -methylacrylate) in DMF.¹⁰² These studies revealed mechanistic aspects of the aryl triflate activation in highly polar, coordinating solvents and in the presence of added coordinating anions. However, these studies did not show how aryl triflates add in nonpolar solvents. Additions of aryl triflates in nonpolar solvents initiate the reactions between aryl triflates and many heteroatom and carbon nucleophiles developed recently in our lab and others.^{94,114–116}

We have previously studied the oxidative addition of aryl bromides to Pd(BINAP)₂ (**1**).⁹⁹ Ligand dissociation from **1** was the rate-limiting step of the oxidative addition of ArBr to **1** and in the catalytic reaction of aryl bromides with primary amines catalyzed by **1**.

(109) Jutand, A.; Mosleh, A. *Organometallics* **1995**, *14*, 1810–1817.

(110) Ludwig, M.; Strömberg, S.; Svensson, M.; Åkermark, B. *Organometallics* **1999**, *18*, 970–975.

(111) Hii, K. K.; Caridge, T. D. W.; Brown, J. M. *Angew. Chem., Int. Ed. Engl.* **1997**, *36*, 984–987.

(112) Brown, J. M.; Perez-Torrente, J. J.; Alcock, N. W.; Clase, H. *J. Organometallics* **1995**, *14*, 207–213.

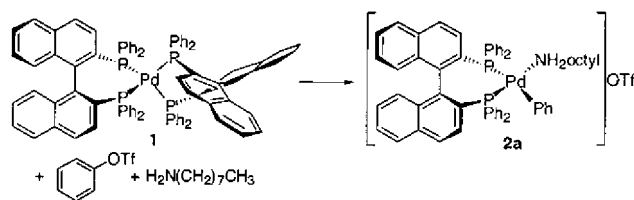
(113) Stang, P. J.; Kowalski, M. H.; Schiavelli, M. D.; Longford, D. *J. Am. Chem. Soc.* **1989**, *111*, 3347–3346.

(114) Ozawa, F.; Kubo, A.; Hayashi, T. *J. Am. Chem. Soc.* **1991**, *113*, 1414–1419.

(115) Wolfe, J. P.; Buchwald, S. L. *J. Org. Chem.* **1997**, *62*, 1264–1267.

(116) Louie, J.; Driver, M. S.; Hamann, B. C.; Hartwig, J. F. *J. Org. Chem.* **1997**, *62*, 1268–1273.

Scheme 1



These reactions typically occurred at 70°C over the course of about 2 h.⁹⁹ These results implied that the same maximum rate would be observed for reactions of aryl halides or triflates using BINAP-ligated palladium as catalyst. However, room-temperature amination reactions have been reported with aryl iodides.¹¹⁷ The rates for catalytic amination of aryl triflates, relative to bromides and iodides, vary with metal complex,¹⁰⁰ but the amination of aryl triflates occurred with rates similar to the amination of aryl bromides when catalyzed by Pd(0) ligated by DPPF or BINAP.^{115,116} Although the Pd(0) species in reactions catalyzed by the combination of Pd₂(dba)₃ and BINAP and by Pd(BINAP)₂ may be different we also considered that aryl iodides could react by a different mechanism than do aryl bromides. To investigate the mechanistic origin of the faster rates for catalytic reactions of aryl iodides, we studied the mechanism for oxidative addition of aryl iodides and triflates to Pd(BINAP)₂.

Here we report distinct mechanistic features for oxidative addition of aryl iodides and triflates vs aryl bromides. The isolation and full characterization of the amine-ligated product from addition of aryl triflate, [(BINAP)Pd(Ar)(H₂NR)]OTf, allowed for a detailed kinetic study of the oxidative addition of ArOTf to Pd(BINAP)₂. Because this amine-ligated species is a crucial intermediate in the amination of aryl triflates, its reactivity with bases to form free amine products was also studied. Moreover, we report its structural determination by single-crystal X-ray diffraction, which provides an unusual example of a structurally characterized product from aryl triflate oxidative addition.

Results

Oxidative Addition of ArOTf to Pd(BINAP)₂ and Synthesis of [(BINAP)Pd(Ar)(H₂NR)]OTf (2**).** Reaction of phenyl triflate alone with **1** at 50°C led to the formation of several reaction products. To determine the spectroscopic features of the addition product, [(BINAP)Ph(Ph)Br] was treated with silver trifluoromethanesulfonate in THF or acetonitrile at room temperature. However, this reaction, again, generated a mixture of several phosphine-containing complexes, none of which displayed in the ³¹P{¹H} NMR spectrum the appropriate AB pattern for [(BINAP)Pd(Ph)OTf]. Finally, we attempted to trap the oxidative addition product [(BINAP)Pd(Ph)OTf] with amine, which would generate an intermediate important in the amination of aryl triflates.

To do so, we conducted the reaction between phenyl trifluoromethanesulfonate and Pd(BINAP)₂ in the presence of 5 equiv of *n*-octylamine (Scheme 1). At 50°C the reaction proceeded smoothly to generate a single AB

(117) Wolfe, J. P.; Buchwald, S. L. *J. Org. Chem.* **1997**, *62*, 6066–6068.

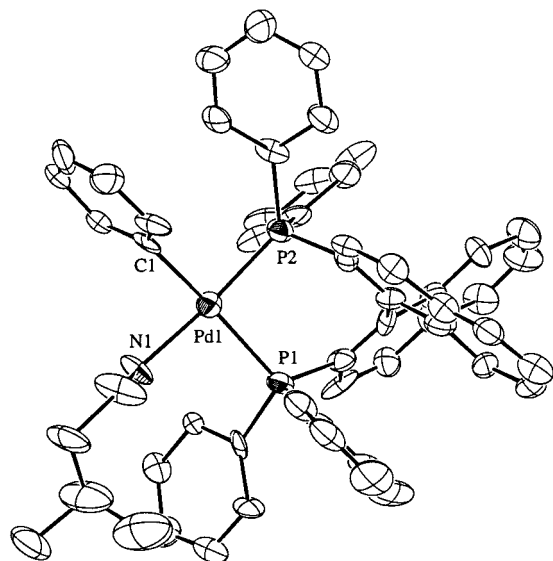
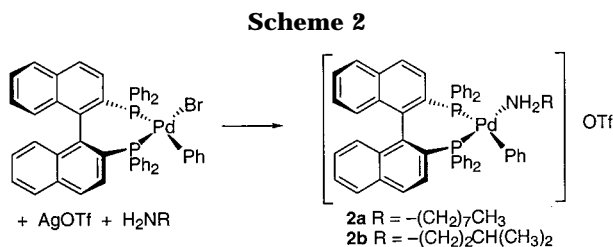


Figure 1. ORTEP drawing of [(BINAP)Ph(Ph)(H₂N(CH₂)₂-CH(CH₃)₂)OSO₂CF₃], **2b**. Hydrogen atoms and triflate counterion omitted for clarity.



pattern in the ³¹P{¹H} NMR spectrum without the detection of any intermediates. The compound formed from the oxidative addition of aryl triflate in the presence of *n*-octylamine was assigned as [(BINAP)Pd(Ph)(H₂N(CH₂)₇CH₃)]OSO₂CF₃ (**2a**) based on spectroscopic data. Diastereotopic amine NH₂ resonances were observed at 3.24 and 3.44 ppm in the ¹H NMR spectrum, and the triflate counterion displayed ν_{SO} bands at 816 and 1284 cm⁻¹ corresponding to a free triflate.¹¹⁸ This material was synthesized independently by treating a suspension of (BINAP)Pd(Ph)Br in toluene with *n*-octylamine and 1 equiv of silver trifluoromethanesulfonate (Scheme 2). Single crystals suitable for an X-ray diffraction study were obtained by recrystallizing this material from toluene and pentane. However, the *n*-octyl chain of the primary amine ligand was severely disordered, and a final refinement of the structure was not achieved. {(BINAP)Pd(Ph)[H₂N(CH₂)₂CH(CH₃)₂]}OTf (**2b**) was synthesized by treating a CH₂Cl₂ solution of (BINAP)Pd(Ph)Br and isoamylamine with silver trifluoromethanesulfonate. Crystallization of the resulting CH₂Cl₂ solution by addition of toluene and heptane produced single crystals of **2b** suitable for X-ray diffraction. An ORTEP plot of **2b** is shown in Figure 1. The P1–Pd1–P2 angle is 90.8°, which is the smallest bite angle known for BINAP complexes of the nickel triad (91.3–95.8°).^{94,119–130} The sum of the angles around

Pd is 360.1°. The phenyl group bound to palladium describes a 101° dihedral angle with the plane defined by N1, Pd1, and C1. Although the hydrogen atoms of the NH₂ group were not located, 2.266 Å was found to be the closest distance between the oxygens of the triflate counterion and the NH₂ hydrogens placed at idealized positions. This distance suggests the possibility of hydrogen bonding between the triflate and the NH protons of the coordinated amine ligand. The Pd–P bond lengths differ by 0.142 Å (P1–Pd1 2.401 Å; P2–Pd1 2.259 Å). The longer bond is trans to the phenyl ligand. The Pd1–P2 bond distance is within the range of distances reported for monocationic BINAP complexes of palladium(II) (2.183–2.332 Å).^{121,122,124–126,128,129} The Pd1–P1 bond distance is longer than the Pd–P bond lengths measured in the reports above, but it is shorter than the longest Pd–P distance found in [(*R*)-*p*-Tol-BINAP]Pd(*p*-C₆H₄-CN)(Br), also corresponding to phosphorus trans to the aryl ligand.¹²⁰

Mechanism of Oxidative Addition of Aryl Triflates and Aryl Iodides to Pd(BINAP)₂. Aryl Triflate Additions. Rate constants for oxidative addition of PhOTf to Pd(BINAP)₂ were determined from plots of the disappearance of the absorbance band at 519 nm corresponding to Pd(BINAP)₂. Rate constants were obtained at 45 °C in the presence of amine to trap the triflate addition product. The reaction solutions contained 2.25 × 10⁻⁵ M Pd(BINAP)₂, 2.26 × 10⁻⁴ to 1.36 M PhOTf, 1.70 × 10⁻⁴ to 6.78 × 10⁻⁴ M BINAP, and 1.13 × 10⁻⁴ M of *n*-octylamine. A typical plot for the decay of Pd(BINAP)₂ vs time is shown in Figure 2. There was no dependence of *k*_{obs} on the concentration of added *n*-octylamine: reactions with a concentration of PhOTf equal to 2.26 × 10⁻⁴ M and amine concentrations ranging from 1.13 × 10⁻⁴ to 1.13 × 10⁻³ M gave rate constants within 15% of each other. Although Pd(BINAP)₂ is consumed by reaction with PhOTf with or without added amine, we were not able to obtain reproducible rate constants for the disappearance of Pd(BINAP)₂ in the absence of *n*-octylamine. Many unidentified ¹H and ³¹P{¹H} resonances were observed, and the reaction turned a dark orange-brown color. Thus, it was unclear what reaction corresponded to the rate being measured in the absence of added amine.

The dependence of the reaction rate constant on [BINAP] was measured with a 2.26 × 10⁻⁴ M concentration of PhOTf and a 1.13 × 10⁻⁴ M concentration of amine. A plot of 1/*k*_{obs} vs [BINAP], shown in Figure 3,

(121) Kuwano, R.; Ito, Y. *J. Am. Chem. Soc.* **1999**, *121*, 3236–3237.

(122) Fujii, A.; Hagiwara, E.; Sodeoka, M. *J. Am. Chem. Soc.* **1999**, *121*, 5450–5458.

(123) Alcock, N. W.; Brown, J. M.; Perez-Torrente, J. J. *Tetrahedron Lett.* **1992**, *33*, 389–392.

(124) Pregosin, P. S.; Ruegger, H.; Salzmann, R.; Albinati, A.; Lianza, F.; Kunz, R. W. *Organometallics* **1994**, *13*, 83–90.

(125) Sodeoka, M.; Tukunoh, R.; Miyazaki, F.; Hagiwara, E.; Shibasaki, M. *Synlett* **1997**, *5*, 463.

(126) Drommi, D.; Nesper, R.; Pregosin, P. S.; Trabesinger, G.; Zurcher, F. *Organometallics* **1997**, *16*, 4268–4275.

(127) Wicht, D. K.; Zhuravel, M. A.; Gregush, R. V.; Glueck, D. S.; Guzei, I. A.; Liable-Sands, L. M.; Rheingold, A. L. *Organometallics* **1998**, *17*, 1412–1419.

(128) Yamaguchi, M.; Yabuki, M.; Yamaishi, T.; Sakai, T.; Tsubomura, T. *Chem. Lett.* **1996**, *3*, 241–242.

(129) Pregosin, P. S.; Ruegger, H.; Salzmann, R.; Albinati, A.; Lianza, F.; Kunz, R. W. *Organometallics* **1994**, *13*, 5040–5048.

(130) 3D Search and Research Using the Cambridge Structural Database Allen, F. H.; Kennard, O. *Chem. Des. Automation News* **1993**, *8*, 31–37.

(118) Lawrance, G. A. *Chem. Rev.* **1986**, *86*, 17–33.

(119) Tominaga, H.; Sakai, K.; Tsubomura, T. *J. Chem. Soc., Chem. Commun.* **1995**, 2273–2274.

(120) Drago, D.; Pregosin, P. S.; Tschoerner, M.; Albinati, A. *J. Chem. Soc., Dalton Trans.* **1999**, 2279–2280.

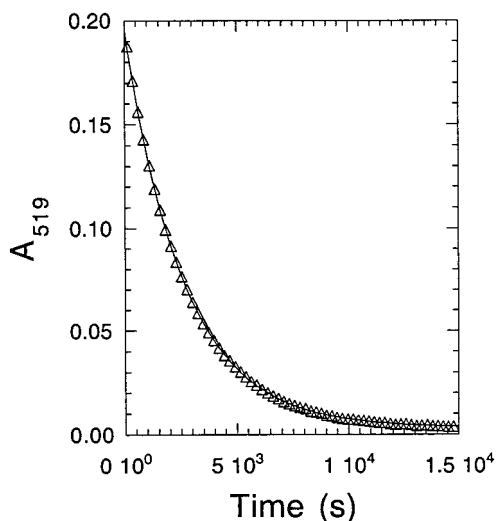


Figure 2. Typical decay of **1** during the reaction of phenyl triflate with **1** at 45 °C in benzene solvent.

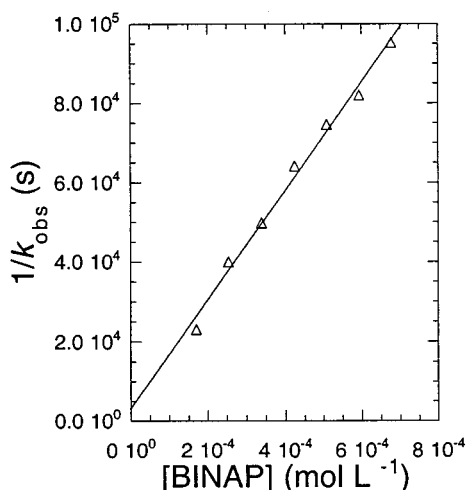


Figure 3. Order in [BINAP] for the reaction of phenyl trifluoromethanesulfonate with **1**.

indicates a linear relationship between rate constant and free ligand concentration. The dependence of the reaction rate on [PhOTf] was measured at a constant 1.70×10^{-4} M concentration of added BINAP. Figure 4 shows that the reaction is first-order in [PhOTf] at low [PhOTf], but that the reaction rate is independent of [PhOTf] at high [PhOTf]. Increasing the concentration of PhOTf beyond 0.2 M had no further effect on the rate of the reaction. To probe for solvent effects, reactions were performed with [PhOTf] of 2.26×10^{-4} M in THF, 2,5-dimethyl THF, and mesitylene solvent. These data are summarized in Table 3. The rate constants obtained in these solvents were nearly identical to each other and to the rate constant for reaction in benzene. Rate constants for reactions conducted in the presence of tetraoctylammonium chloride, tetraoctadecylammonium bromide, tetrabutylammonium triflate, or tetrabutylammonium hexafluorophosphate were within experimental error of rate constants obtained for reactions conducted in the absence of these additives (Table 3). $^{31}\text{P}\{^1\text{H}\}$ NMR analysis of these reactions indicated that (BINAP)Pd(Ph)X (X = Cl, Br) complexes were formed instead of **2a** when the reaction was conducted with tetraoctylammonium chloride and tetraoctadecylammo-

num bromide. No difference between the $^{31}\text{P}\{^1\text{H}\}$ resonances of the reaction product and those of **2a** were observed when the reactions were run in the presence of added tetrabutylammonium triflate or hexafluorophosphate.

Aryl Iodide Additions. The oxidative addition of aryl iodides to Pd(0) usually proceeds faster than the oxidative addition of aryl bromides and chlorides. Indeed, qualitative studies on the oxidative addition of iodobenzene to Pd(BINAP)₂ showed that the reaction did proceed faster than the addition of bromobenzene. This result appeared to contradict our results, presented in the Introduction, regarding the zero-order dependence on aryl bromide concentration for the oxidative addition of ArBr to **1**.¹¹⁷ Naturally, reaction rates that are zero-order in substrate should also be independent of the identity of the substrate.

To understand this apparent contradiction, we conducted quantitative kinetic studies on the addition of aryl iodides to **1**. Rate constants for oxidative addition of PhI to Pd(BINAP)₂ were measured by UV-vis spectroscopy. The reactions were performed at 40 °C. Typically, reaction mixtures contained 8.55×10^{-7} to 2.25×10^{-5} M Pd(BINAP)₂. Concentrations of ArI ranged from 8.94×10^{-7} to 4.20 M, and concentrations of BINAP ranged from 3.39×10^{-6} to 1.70×10^{-4} M. A typical plot of the decay of Pd(BINAP)₂ vs time is shown in Figure 5. The dependence of the reaction rate constant on [BINAP] was measured using a concentration of phenyl iodide (1.79×10^{-6} M) that lies within the range of concentrations that produced a first-order dependence on PhI (see below). A plot of $1/k_{\text{obs}}$ vs [BINAP], presented in Figure 6, shows a linear relationship between these quantities. The dependence of the reaction rate on [PhI] was measured with [BINAP] equal to 1.70×10^{-4} M. Figure 7 shows that for the concentration range of 3.35×10^{-6} to 2.00×10^{-2} M the rate constant displayed saturation behavior.

However, k_{obs} was not completely independent of [PhI], as revealed by increasing the concentration of phenyl iodide far beyond 2.50×10^{-2} M. Rate constants as a function of [PhI] at high concentrations of PhI are shown in Figure 8. NMR spectroscopic studies showed that reactions occurred in high yield at these high concentrations of aryl iodide; the decay of Pd(BINAP)₂ was not accelerated by a side reaction that also consumed Pd(BINAP)₂. No biaryl side products were detected by analyzing reactions containing high concentrations of PhI by GC/MS. These data argue against an electron transfer mechanism that generates freely diffusing σ -phenyl radicals. Reactions conducted with iodobenzene that was freshly distilled from sodium bisulfite, CaH₂, and KOH to remove H₂O, HI, and I₂ impurities occurred with the same rate constants as those conducted with PhI that was used directly from a commercial supplier. No measurable accumulation of an adduct of the ArI with the starting Pd(BINAP)₂ was detected by ^1H or $^{31}\text{P}\{^1\text{H}\}$ NMR spectroscopy.

To probe for a medium effect that may result from changes in solvent polarity at these high concentrations of PhI, reactions were performed with [PhI] of 3.50×10^{-3} M and increasing amounts of added chlorobenzene. Chlorobenzene is more polar than PhI and does not react with **1**. Reactions with concentrations of PhCl as

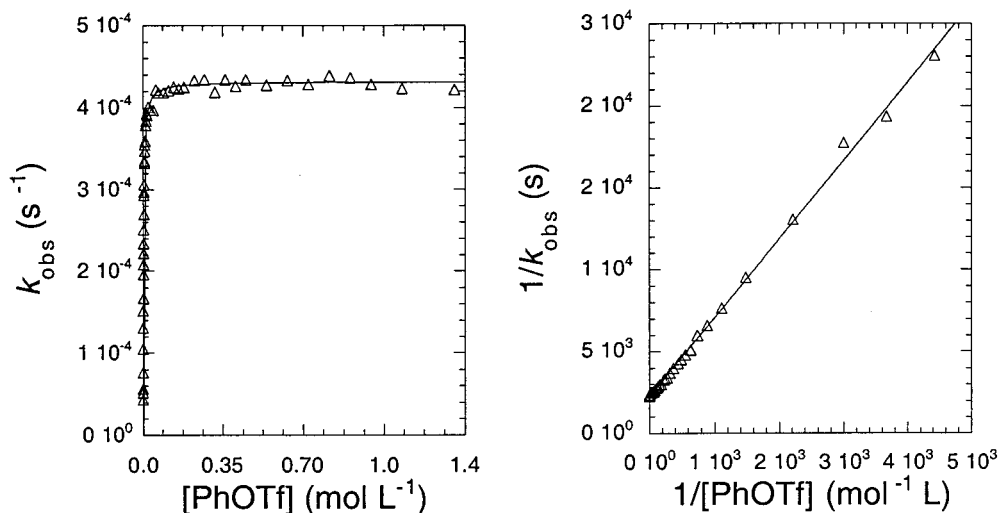


Figure 4. Order in [PhOTf] for the reaction of phenyl trifluoromethanesulfonate with **1**.

Table 1. Intramolecular Bond Distances (Å) and Angles (deg) for 2b

Pd(1)–P(1)	2.401(1)	Pd(1)–P(2)	2.259(4)
Pd(1)–N(1)	2.09(1)	Pd(1)–C(1)	2.00(2)
P(1)–Pd(1)–P(2)	90.8(1)	P(1)–Pd(1)–N(1)	92.7(3)
P(2)–Pd(1)–C(1)	91.8(4)	N(1)–Pd(1)–C(1)	84.8(5)
P(1)–Pd(1)–C(1)	175.1(6)	P(2)–Pd(1)–N(1)	176.4(3)

Table 2. Data Collection and Refinement Parameters for the X-ray Structure of [(BINAP)Pd(Ph)(H₂N(CH₂)₂CH(CH₃)₂)OTf (2b)]

empirical formula	C ₅₆ H ₅₀ NO ₃ F ₃ P ₂ SPd·0.75(C ₇ H ₁₆)
fw	1117.57
cryst color, habit	colorless, plate
cryst dimens	0.08 × 0.10 × 0.13 mm
cryst syst	monoclinic
lattice type	primitive
lattice params	<i>a</i> = 11.013(1) Å <i>b</i> = 16.361(1) Å <i>c</i> = 15.481(1) Å <i>β</i> = 94.024(4)°
volume	2782.5(3) Å ³
space group	<i>P</i> 2 ₁ (#4)
<i>Z</i> value	2
diffractometer	Nonius KappaCCD
radiation	Mo Kα (<i>λ</i> = 0.71069 Å) graphite monochromated
<i>T</i>	−90.0 °C
residuals	<i>R</i> ; <i>R</i> _w 0.055; 0.050
goodness-of-fit indicator	1.59

Table 3. Effect of Solvent and Additives on the Oxidative Addition of PhOTf to 1

solvent	<i>k</i> _{obs} × 10 ⁵ s ^{−1}	additive (THF solvent)	<i>k</i> _{obs} × 10 ⁵ s ^{−1}
benzene	4.3 (±0.3) ^a	<i>N</i> (<i>n</i> -Bu) ₄ OTf	4.58
THF	4.21	<i>N</i> [<i>n</i> -(CH ₂) ₇ (CH ₃) ₄]Cl	4.41
2,5-dimethyl-THF	2.44	<i>N</i> [<i>n</i> -(CH ₂) ₁₇ (CH ₃) ₄]Br	4.38
mesitylene	2.61	<i>N</i> (<i>n</i> -Bu) ₄ PF ₆	4.68

^a The relative errors in rate constants were similar in all cases and were estimated from duplicate and in some cases triplicate runs under identical conditions.

high as 4.00 M showed only a modest increase in rate constant (filled circles in Figure 8). In addition, there was no dependence of *k*_{obs} in THF solvent on added NBu₄PF₆ (Table 4), which would also change solvent polarity. The reaction rate constant also did not change

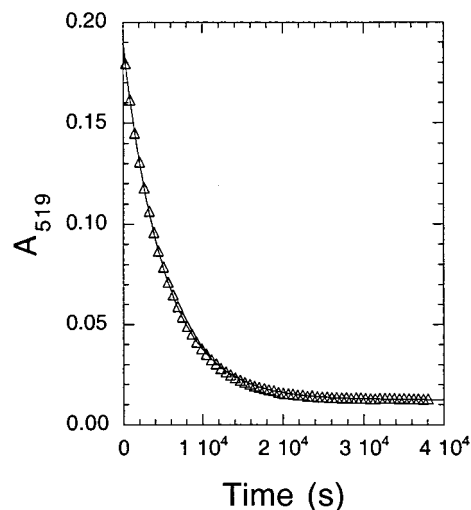


Figure 5. Typical decay of **1** during the reaction of phenyl iodide with **1** at 45 °C in benzene solvent.

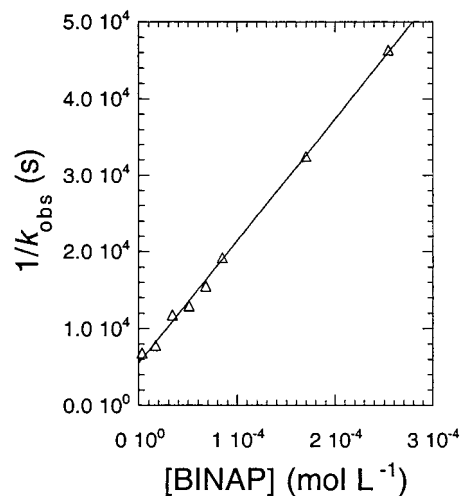


Figure 6. Order in [BINAP] for the reaction of **1** with phenyl iodide.

appreciably with a complete change in medium. At 4.15 × 10^{−6} M [PhI] and 6.24 × 10^{−6} M [BINAP], the rate constants were within a factor of 4 when obtained in benzene, THF, and 2,5-dimethyl THF solvent (Table 4).

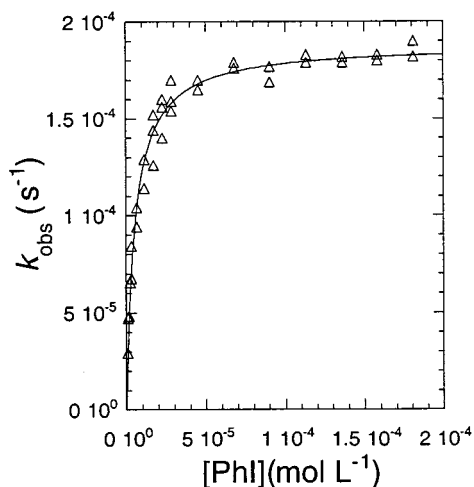


Figure 7. Order in [PhI] for the reaction of **1** with phenyl iodide for [PhI] < 2.0×10^{-4} M.

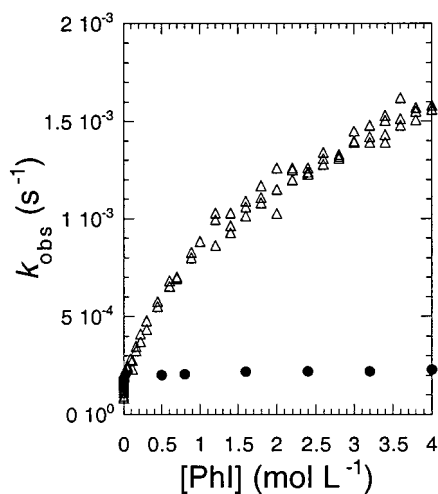


Figure 8. Dependence of k_{obs} on [PhI] for the reaction of **1** with phenyl iodide for [PhI] < 4.0 M (triangles). Dependence of k_{obs} on increasing [PhCl] at [PhI] of 3.50×10^{-3} M (circles).

Table 4. Effect of Solvent and Additives on the Oxidative Addition of PhI to 1

solvent	$k_{\text{obs}} \times 10^4 \text{ s}^{-1}$	additive	$k_{\text{obs}} \times 10^4 \text{ s}^{-1}$
benzene	1.63 (± 0.1)	<i>n</i> -octylamine	1.83
THF	0.45	(benzene solvent)	
2,5-dimethyl-THF	0.43	N(<i>n</i> -Bu) ₄ PF ₆ (THF solvent)	0.27

Finally, there was no dependence on added amine (Table 4) that would be present in catalytic aryl halide amination.

Addition of Aryl Bromides at High [PhBr]. Having observed an effect of [ArI] on reaction rate at high concentrations of aryl iodide, we measured rate constants for the addition of PhBr to Pd(BINAP)₂ at concentrations up to 3.20 M. Rate constants were obtained at 45 °C by UV-vis spectroscopy. The reactions contained 2.25×10^{-5} M Pd(BINAP)₂, 1.70×10^{-4} M BINAP, and concentrations of PhBr ranging from 0.50 to 3.20 M. Figure 9 shows these new data along with those published previously.⁹⁹ These results showed that there is again an increase in rate with these large increases in ArX concentration. However, there was only a modest increase in the rate of oxidative addition

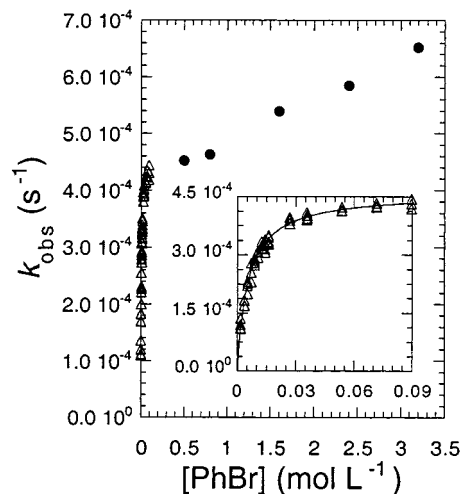


Figure 9. Dependence of k_{obs} on [PhBr] for the reaction of **1** with phenyl bromide for [PhBr] 0.50–3.20 M (circles) and 1.78×10^{-3} to 89.5×10^{-3} M (triangles, inset).

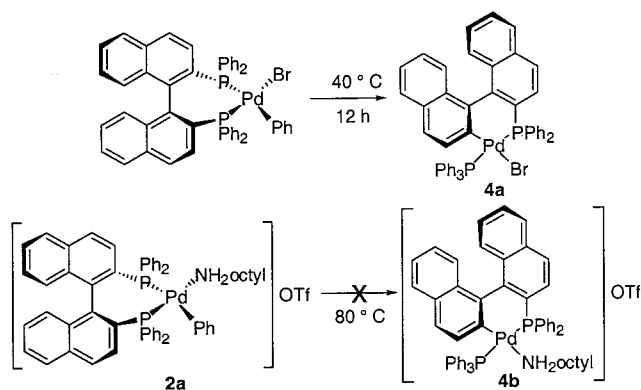
beyond that measured at concentrations where k_{obs} is nearly zero-order in [PhBr]. These data stand in contrast to the large increase in k_{obs} for reactions with the high concentrations of iodobenzene.

Reactivity of [(BINAP)Pd(Ar)(H₂NR)]OTf (**2a**).

To test the competence of the amine-ligated aryl triflate complex [(BINAP)Pd(Ph)(H₂N(CH₂)₇CH₃)]OSO₂CF₃ as an intermediate in the catalytic amination of aryl triflates, we treated solutions of **2a** in C₆D₆ or C₇D₈ containing 2 equiv of free BINAP with several bases. Addition of NaO-*t*-Bu to **2a** generated *N*-octylaniline and Pd(BINAP)₂ in quantitative yield at room temperature. Addition of cesium carbonate or potassium phosphate, which have been reported to be superior bases for the amination of aryl triflates,¹¹⁵ to a suspension of **2a** in toluene-*d*₈ at room temperature led to no reaction. However, heating and vigorously stirring the suspension of Cs₂CO₃ in a toluene-*d*₈ solution of **2a** for 7 h at 50 °C generated *N*-octylaniline in 97% yield. Reaction of **2a** with K₃PO₄ was slower and occurred only after heating for 18 h at 50 °C (94% yield of *N*-octylaniline). For comparison, Cs₂CO₃ was suspended and stirred in a C₆D₆ solution of (BINAP)Pd(Ph)Br, *n*-octylamine, and 2 equiv of BINAP. No reaction was observed after 2 h at room temperature. Prolonged heating of the reaction mixture at 50 °C generated free PPh₃ and no *N*-octylaniline, indicating that cleavage of the P–C bond of the BINAP ligand backbone⁹⁹ is faster than the formation of an aryl amido complex from (BINAP)Pd(Ph)Br, *n*-octylamine, and Cs₂CO₃ under these conditions.

Complexes of the formula (BINAP)Pd(Ar)Br have been shown to undergo P–C bond cleavage to form **4a** (Scheme 3).⁹⁹ In contrast, **2a** was stable for greater than 8 h at 60 °C. Heating of **2a** at 80 °C for 3 h did lead to the onset of decomposition. This thermolysis generated several products, but none of the products could be assigned to a cationic, amine-ligated P–C cleaved complex **4b** (Scheme 3). Moreover, addition of DMPE (1,2-bis(dimethylphosphino)ethane) to the reaction mixture did not liberate PPh₃ as it did after thermolysis of BINAP-ligated arylpalladium halide complexes. Thus, P–C cleavage did not occur during the thermal decom-

Scheme 3



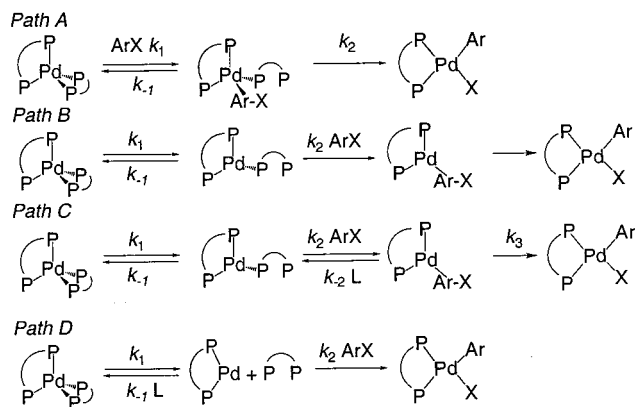
position of **2a**. No *N*-octylaniline was detected by GC/MS analysis of the reaction mixture.

Discussion

Preparation and Reactivity of [(BINAP)Pd(Ar)(H₂NR)](OTf). Studies on the oxidative addition of aryl triflates to Pd(0) ligated by chelating bisphosphines have been hampered by the instability of the resulting [LPdArY]⁺OTf⁻ complexes. In the past, the oxidative addition product has been trapped by added anions such as Cl⁻, I⁻, or AcO⁻ to form stable (DPPF)Pd(Ar)X complexes.¹⁰² Ludwig and Åkermark reported the preparation of several arylpalladium triflate complexes ligated by dppp, dppe, dcpe, and dppt (1,3-bis(diphenylphosphino)propane, 1,2-bis(diphenylphosphino)ethane, 1,2-bis(dicyclohexylphosphino)ethane, and (*Z*)-1,2-bis(diphenylphosphino)ethylene).¹¹⁰ In this report, the complexes were generated in situ by reaction of the corresponding iodo complexes with silver triflate, but the triflate complexes were not isolated. Jutand and Mosleh reported the oxidative addition of aryl triflates to Pd(PPh₃)₄.¹⁰⁹ They monitored by electrochemical techniques the decay of Pd(0) and the appearance in DMF of a new conducting complex. They also reported the synthesis and isolation of two PPh₃-ligated arylpalladium trifluoromethanesulfonate complexes. These complexes contained coordinated CH₂Cl₂ and were handled in solutions of strongly coordinating solvents such as acetone and DMF. While these studies provide information on catalytic reactions that are commonly run in DMF solvent or in the presence of added coordinating anions, such as the Heck reaction, they are less informative about the oxidative addition in the amination chemistry that is conducted in noncoordinating, less polar solvents. In general, the amination chemistry does not occur in polar solvents such as NMP or DMF,¹³¹ and the addition of halide salts inhibits the reaction of aryl triflates with amines when bisphosphines are used.^{115,116}

Reaction of PhOTf with a toluene solution of Pd-(BINAP)₂ containing 5 equiv of *n*-octylamine or reaction of (BINAP)Pd(Ph)Br with silver trifluoromethanesulfonate in toluene in the presence of *n*-octylamine resulted in the clean formation of the likely catalytic intermediate [(BINAP)Pd(Ph)(H₂N(CH₂)₇CH₃)]OTf (**2a**). Indeed, [(BINAP)Pd(Ph)(H₂N(CH₂)₇CH₃)]OTf reacted

Scheme 4



cleanly with bases in the presence of added BINAP to afford *N*-octylaniline and Pd(BINAP)₂. Although **2a** reacted with weak, insoluble bases only upon heating, it did react faster than [(BINAP)Pd(Ar)(Br)] with amine and Cs₂CO₃ under identical conditions.^{115,132}

Mechanism of Oxidative Addition of ArX to Pd-(BINAP)₂. Potential mechanisms for the oxidative addition of aryl halides and sulfonates to Pd(BINAP)₂ are shown in Scheme 4. Path A involves the reversible associative displacement of an arm of the bisphosphine by the aryl halide or sulfonate electrophile, followed by rate-limiting C-X bond scission by the resulting coordinatively saturated 18-electron Pd(0) complex. The rate law for this mechanism predicts a reaction that is first-order in Ar-X and zero-order in added ligand (eq 1). Path B depicts a mechanism in which one arm of the

Path A:

$$k_{\text{obs}} = \frac{k_1 k_2 [\text{ArX}]}{k_{-1} + k_2} \quad (1)$$

coordinated BINAP undergoes reversible dissociation to create an open coordination site. Irreversible coordination of Ar-X and cleavage of the C-X bond follows this preequilibrium. This path would show a zero-order dependence of rate on free ligand concentration and a variable dependence of k_{obs} on [ArX]. The rate law derived from this mechanism (eq 2) shows that the

Path B:

$$k_{\text{obs}} = \frac{k_1 k_2 [\text{ArX}]}{k_{-1} + k_2 [\text{ArX}]} \frac{1}{k_{\text{obs}}} = \frac{1}{k_1} + \frac{k_{-1}}{k_1 k_2 [\text{ArX}]} \quad (2)$$

reaction can display zero-order behavior in [ArX] at high concentration of aryl halide or sulfonate. This zero-order behavior arises when the $k_2 [\text{ArX}]$ term in the denominator becomes much larger than k_{-1} . Path C is similar to the mechanism in path B, except that coordination of aryl halide or triflate is reversible. This mechanism would reversibly generate a Pd(0) complex containing both a chelating BINAP and an intact, coordinated Ar-X through a combination of dissociative and associative steps. The rate law for this mechanism (eq 3) predicts reaction orders similar to those predicted by

(131) Louie, J.; Paul, F.; Hartwig, J. F. *Organometallics* **1996**, *15*, 2794–2805.

(132) Wolfe, J. P.; Buchwald, S. L. *Tetrahedron Lett.* **1997**, *38*, 6359–6362.

Path C:

$$k_{\text{obs}} = \frac{k_1 k_2 k_3 [\text{ArX}]}{k_{-1} k_3 + k_{-1} k_2 [\text{L}] + k_2 k_3 [\text{ArX}]} \quad \frac{1}{k_{\text{obs}}} = \frac{1}{k_1} + \frac{k_{-1}}{k_1 k_2 [\text{ArX}]} + \frac{k_{-1} k_2 [\text{L}]}{k_1 k_2 k_3 [\text{ArX}]}$$

$$k_{\text{obs}} = \frac{k_1 k_2 k_3 [\text{ArX}]}{k_{-1} k_3 + k_{-1} k_2 [\text{L}] + k_2 k_3 [\text{ArX}]} = k_1 \quad \text{when } [\text{ArX}] \gg [\text{L}] \quad (3)$$

path D. Path D involves the full, reversible dissociation of a chelating ligand to generate the 14-electron intermediate (BINAP)Pd, which undergoes irreversible oxidative addition of aryl halide or triflate. The rate law corresponding to path D is shown in eq 4. This rate

Path D:

$$k_{\text{obs}} = \frac{k_1 k_2 [\text{ArX}]}{k_{-1} [\text{L}] + k_2 [\text{ArX}]} \quad \frac{1}{k_{\text{obs}}} = \frac{1}{k_1} + \frac{k_{-1} [\text{L}]}{k_1 k_2 [\text{ArX}]}$$

$$k_{\text{obs}} = \frac{k_1 k_2 [\text{ArX}]}{k_{-1} [\text{L}] + k_2 [\text{ArX}]} = k_1 \quad \text{when } [\text{ArX}] \gg [\text{L}] \quad (4)$$

equation predicts an inverse first-order dependence of reaction rate on free ligand concentration and a first-order dependence on [ArX] when the ratio of [ArX] to [L] (L = BINAP) is low. However, this rate law predicts zero-order behavior in both [ArX] and [L] at high ratios of [ArX] to [L]. For our reactions of aryl triflates in the presence of amine, all four paths involve fast trapping of the (BINAP)Pd(Ar)OTf intermediate by amine. This trapping of the aryl triflate addition product would have no effect on the rate of oxidative addition. Indeed, the reaction rates were zero-order in the concentration of added amine.

No single mechanism accounts for all of our data. Instead, a combination of mechanism D and either mechanism B or C is consistent with our rate measurements. Our data rule out paths A and B as the mechanism for addition of aryl triflates and as the mechanism for addition of aryl iodides and bromides at modest concentrations of the aryl halides. Path A is inconsistent with the zero-order dependence of k_{obs} observed at high [ArX]. Moreover, both paths A and B are inconsistent with the inverse first-order dependence on ligand concentration observed for reactions run at modest concentrations of ArX.

Paths C and D are most consistent with the observed first-order rate dependence on [ArX] at low concentrations, zero-order rate dependence at high [ArOTf], zero-order rate dependence on [ArX] for reactions of aryl bromides and iodides up to about 0.1 M, and inverse first-order dependence on [BINAP] at modest ArX concentrations. We favor path D over path C for reactions of aryl triflates and for reactions of aryl halides at modest concentrations of [ArX]. It seems likely that, at these concentrations of aryl halide or triflate, the recoordination of a ligand arm would be faster than intermolecular coordination of the weakly donating aryl electrophile. Yet, reaction by exclusively path C or D at all concentrations of aryl halide is inconsistent with the increase in k_{obs} observed when the concentration of ArI and ArBr was above 1 M.

Thus, we probed whether the increase in rate constant with such high concentrations of aryl halide substrate

could be due to solvent polarities or reagent impurities rather than the onset of a second, concurrent mechanism. At the highest concentrations of iodobenzene, this reagent accounted for more than 50% of the sample volume. However, replacing the iodobenzene with chlorobenzene, which is an unreactive haloarene with a greater dielectric constant, provided only modest increases in k_{obs} . Extraneous consumption of Pd(BINAP)₂ by contaminants in the PhI, such as I₂, HI, or H₂O, was ruled out by observing similar rates for oxidative addition when using commercial PhI as received and when using purified PhI. Thus, solvent polarity or reagent impurities do not account for the increase in rate at high concentrations of ArX.

Instead, we propose that a second mechanism, which is faster for iodides than bromides and does not occur at all when using aryl triflates, operates at high concentrations of ArX. The dependence of k_{obs} at high [PhI] is clearly positive, but is not strictly linear. Nonideal solution behavior of substrate may lead to this curvature at the highest concentrations of aryl halide. This second mechanism must involve reaction of the metal with ArX before the irreversible step. This mechanism cannot involve full dissociation of ligand because full dissociation of ligand is slower than the overall reaction at high [ArI]. This reaction could involve coordination or addition of the ArX to the 16-electron palladium metal center formed by partial ligand dissociation, as shown in pathway B or C of Scheme 4. At the concentrations of ArX that approach those of solvent, coordination of ArX may compete with reassociation of an arm of the partially dissociated BINAP. Alternatively, an electron transfer mechanism may begin to operate at high ArX. This mechanism may involve an electron transfer that is first-order in both palladium and ArX reagent and that occurs prior to dissociation of ligand from the metal center. If this mechanism does operate, then it must not form arene or biaryl compounds because the reaction yields are equally high at low or high concentrations of ArX.

Our data do not firmly support addition of the aryl bromide to the 16-electron species over the electron transfer pathway, but we do favor nonradical mechanism B or C. The absence of biphenyl formed at high concentrations of ArX suggests the absence of freely diffusing Ar[•] intermediates. Moreover, the trend in importance of this second mechanism at high ArX as a function of X tracks well with the coordinating ability of the aryl electrophile and less with its electrophilicity. Halocarbon coordination to low-valent late metals is known to be more favorable for iodides than bromides,^{133–139} and complexes of intact alkyl or aryl triflates are unknown. Iodobenzene is a better ligand

(133) Kulawiec, R. J.; Crabtree, R. H. *Coord. Chem. Rev.* **1990**, *99*, 89–115.

(134) Crabtree, R. H.; Mellea, M. F.; Mihelcic, J. M. *Inorg. Synth.* **1990**, *28* (Reagents Transition Met. Complex Organomet. Synth.), 56–60.

(135) Crabtree, R. H.; Mellea, M. F.; Mihelcic, J. M. *Inorg. Synth.* **1989**, *26*, 122–126.

(136) Crabtree, R. H.; Faller, J. W.; Mellea, M. F.; Quirk, J. M. *Organometallics* **1982**, *1*, 1361–1366.

(137) Kulawiec, R. J.; Faller, J. W.; Crabtree, R. H. *Organometallics* **1990**, *9*, 745–755.

(138) Winter, C. H.; Arif, A. M.; Gladysz, J. A. *J. Am. Chem. Soc.* **1987**, *109*, 7560–7561.

(139) Butts, M. D.; Scott, B. L.; Kubas, G. J. *J. Am. Chem. Soc.* **1996**, *118*, 11831–11843.

Table 5. Ratio of k_2/k_{-1} for the Oxidative Addition of ArX to **1**

ArX	$(k_2/k_{-1}) \times 10^3$	k_2 rel
PhOTf	85.2	1.0
PhBr	97.2	1.1
PhI	31600.0	370.9

than bromobenzene because of the higher polarizability of the iodide lone pairs. Phenyl triflate is a poorer donor than aryl halides is to Pd(0) because of the hardness of the triflate oxygens.

Relative Reactivity of ArI, ArBr, and ArOTf. When k_{obs} for oxidative addition of aryl halides to **1** reaches saturation with respect to the concentration of ArX, the rate of the oxidative addition is solely controlled by the rate of ligand dissociation from **1**. In path D, k_1 (eq 4) represents the rate of ligand dissociation from **1**. The different reactivity of the aryl electrophile toward the unsaturated intermediate (BINAP)Pd can be inferred from the relative magnitudes of the rate constant for the bond-breaking step of the mechanism, k_2 . We cannot directly measure k_2 , but we can determine the ratio of k_2/k_{-1} from plots of the dependence of k_{obs} on the concentration of aryl halide or sulfonate using all concentrations of PhOTf, concentrations of PhBr up to 90 mM, and concentrations of PhI up to 0.2 mM. We can compare these ratios for different aryl electrophiles because the rate constant for re-coordination of BINAP to (BINAP)Pd, k_{-1} , is independent of the identity of the aryl electrophile. The more reactive the electrophile, the larger the magnitude of k_2/k_{-1} . Table 5 contains the values of k_2/k_{-1} determined from the data in Figures 4, 7, and the inset of 9. Comparison of the values of k_2/k_{-1} reveals that phenyl triflate is almost exactly as reactive as phenyl bromide, while phenyl iodide is nearly 400 times more reactive than either PhBr or PhOTf. This information further supports our preference for reaction of aryl triflates and aryl halides at modest concentrations by path D, in which the aryl electrophile oxidatively adds to the 14-electron (BINAP)Pd intermediate without prior reversible coordination. Bromobenzene would be expected to compete with an arm of the BINAP ligand for a coordination site more effectively than would phenyl triflate, and reaction of the aryl bromide would, thereby, produce a significantly higher ratio of k_2/k_{-1} than would reaction of PhOTf.¹⁴⁰

Conclusion

We have shown that the oxidative additions of aryl iodides, bromides, and triflates follow the same mechanism at moderate ArX concentrations. However, a second mechanism, which occurs more readily for ArI than for ArBr and not at all for ArOTf, appears to operate at high concentrations of ArX electrophile. In the case of ArI, this mechanism accounts for more than an 8-fold increase in the rate of oxidative addition relative to the rate of ligand dissociation from Pd(0). This phenomenon is likely to account for the ability to conduct aryl iodide aminations at lower temperatures than aryl bromide aminations when using a Pd catalyst ligated by BINAP. For aryl bromides, the increase in

rate at very high [PhBr] is moderate, and only a doubling of the rate constant for oxidative addition is observed with large increases in aryl bromide concentration. No effect of increasing aryl triflate concentrations was observed on the rate for oxidative addition of this substrate. The increase in reactivity for aryl iodides uncovered in this study may be attributed to the coordinating ability or the X group of the aryl electrophile and is consistent with reports on the coordination ability of haloarenes to low-valent late metals.^{133,136,137,139} This increase in reactivity at very high [ArX] suggests that the initial phases of catalytic reactions conducted on a synthetic scale may occur, in part, by a mechanism that operates in parallel to the one identified in our recent study.

Experimental Section

General Considerations. Unless otherwise noted, all manipulations were conducted using standard Schlenk techniques or in an inert atmosphere glovebox. ¹H NMR spectra were obtained on a Bruker Advance DPX-400 MHz, GE QE 300 MHz, GE Ω 500 MHz, or GE Ω 300 MHz Fourier transform NMR spectrometer. ³¹P{¹H} NMR spectra were obtained on the Ω 300 and 500 MHz spectrometers operating at the corresponding frequencies. ¹⁹F{¹H} NMR spectra were recorded on a Bruker Advance DPX-400 MHz Fourier transform NMR spectrometer and referenced to both an external and an internal fluorobenzene standard. ¹H NMR spectra were recorded relative to residual protiated solvent. ³¹P{¹H} NMR spectra were recorded in units of parts per million relative to 85% H₃PO₄ as external standard. ¹⁹F{¹H} spectra were recorded in units of parts per million relative to 1×10^{-2} M fluorobenzene in C₆D₆ as an external standard. UV-vis spectra were collected on a Varian Cary 3E spectrophotometer equipped with a thermostated multicell block. IR spectra were collected on a Midac M-Series FT-IR spectrophotometer. Elemental analyses were performed by Robertson Microlit Laboratories, Inc., Madison, NJ.

All reagents were purchased from commercial suppliers and used without further purification. Pd(BINAP)₂⁹⁹ and (BINAP)-Pd(Ph)Br⁹⁹ were prepared using literature procedures, unless otherwise noted. *n*-Octylamine was heated at reflux over CaH₂ and KOH, distilled under nitrogen, and stored in an inert atmosphere glovebox. Iodobenzene and bromobenzene were heated over sodium sulfite, CaH₂, and KOH under N₂, distilled under vacuum, and stored in an inert atmosphere glovebox. Protiated solvents were heated to reflux and distilled from purple solutions containing sodium benzophenone ketyl under N₂. Deuterated solvents were dried similarly but were collected by vacuum transfer.

Oxidative Addition of PhOTf to Pd(BINAP)₂ in the Presence of Amine. Pd(BINAP)₂ (7 mg, 5.2 μmol) was dissolved in 0.6 mL of THF. The solution was then transferred to a screw-capped NMR tube containing a PTFE-lined septum cap. Prior to sealing the tube, PhOTf (4.2 μL, 5.9 mg, 26.1 μmol) and *n*-octylamine (4.3 μL, 3.3 mg, 25.5 μmol) were added to the solution. An initial ³¹P{¹H} spectrum was taken, and the solution was heated at 65 °C in an oil bath. Intermediate spectra were recorded at 15 and 30 min, and at 3, 14, and 17 h of reaction time.

Oxidative Addition of PhOTf to Pd(BINAP)₂ in the Absence of Amine. Pd(BINAP)₂ (7 mg, 5.2 μmol) was dissolved in 0.6 mL of THF. The solution was then transferred to a screw-capped NMR tube containing a PTFE-lined septum cap. Prior to sealing the tube, PhOTf (4.2 μL, 5.9 mg, 26.1 μmol) was added to the solution. An initial ³¹P{¹H} NMR spectrum was taken, and the solution was heated at 65 °C in an oil bath. Spectra were recorded at 15, 30, and 60 min of reaction time.

(140) The relevant ratio corresponding to path C is actually more complicated and not a ratio but a constant. From eq 3, the proper expression would be $k_{-1}/k_1k_2 + (1 + k_2[L]/k_3)$.

Preparation of [(BINAP)Pd(Ph)(H₂N(CH₂)₇CH₃)]OTf (2a). (BINAP)Pd(Ph)Br (300 mg, 0.34 mmol) was suspended in 10 mL of toluene. While stirring, *n*-octylamine (45.9 mg, 0.36 mmol) was added to the reaction mixture, followed by silver trifluoromethanesulfonate (91.3 mg, 0.36 mmol). A fine white precipitate formed immediately upon addition of AgOTf, and the color of the solution changed from pale yellow to almost colorless. After stirring at room temperature for 5 min, the solution was carefully decanted and filtered through a plug of Celite. The precipitate was extracted with 2 mL of toluene, and the extract was added to the supernatant after filtration through a plug of Celite. The resulting solution was evaporated to 1/10th of the original volume. The toluene solution was layered with pentane and allowed to rest at -34 °C overnight. The white powdered product was isolated by filtration through a medium-porosity fritted funnel (319.4 mg, 87.1% yield). ¹H NMR (400 MHz, C₆D₆): δ 0.747 (m, 4H), 0.862 (t, *J* = 7.2 Hz, 4H), 0.962 (m, 2H), 1.064 (m, 2H), 1.205 (m, 3H), 1.869 (br, 1H), 2.101 (br, 1H), 3.235 (br, 1H), 3.438 (b, 1H), 6.406 (m, 2H), 6.557 (m, 6H), 6.704 (m, 2H), 6.841 (m, 4H), 6.988 (m, 2H), 7.069 (app t, 2H), 7.18–7.27 (m, 4H), 7.409 (m, 6H), 7.619 (app t, 2H), 7.743 (br, 2H), 7.95–8.15 (m, 5H). ³¹P{¹H} (C₆D₆): δ 15.04 (d, *J*_{pp} = 38 Hz), 28.84 (d, *J*_{pp} = 37 Hz). ¹⁹F{¹H} (C₆D₆): -77.21 (s). IR (C₆H₆): 3310 w, 3216 w, 2924 w, 2857 w, 1576 m, 1437 m, 1284 s, 1259 m, 1224 m, 1099m, 816 w, 748 w. Anal. Calcd for C₅₉H₅₆F₃NO₃P₂PdS: C, 65.34; H, 5.20; N, 1.29. Found: C, 65.08; H, 5.35; N, 1.19.

Preparation of [(BINAP)Pd(Ph)(H₂N(CH₂)₂CH(CH₃)₂)]OTf (2b). (BINAP)Pd(Ph)Br (300 mg, 0.34 mmol) was dissolved in 5 mL of CH₂Cl₂. While stirring, isoamylamine (45.9 mg, 0.36 mmol) was added to the reaction mixture, followed by silver trifluoromethanesulfonate (91.3 mg, 0.36 mmol). A fine white precipitate formed immediately upon addition of AgOTf, and the color of the solution changed from pale yellow to almost colorless. After stirring at room temperature for 5 min, the solution was carefully decanted and filtered through a plug of Celite. The precipitate was extracted with 1 mL of CH₂Cl₂, and the extract was added to the supernatant after filtration through a plug of Celite. The resulting solution was evaporated to approximately 1/10th of the original volume. The solution was layered with toluene and allowed to rest at -34 °C for 1 h. Heptane was then carefully layered on the solution. The mixture was allowed to rest at -34 °C overnight. The product was isolated as colorless crystals suitable for X-ray diffraction, which included ~3/4 molecule of heptane per molecule of complex in the crystal lattice. To obtain satisfactory combustion analysis, this material was further recrystallized by allowing a concentrated toluene solution of **2b** to rest at -34 °C overnight. The product was isolated by filtration as a white microcrystalline powder that retained 1/2 molecule of toluene per molecule of complex (319.4 mg, 87.1% yield). ¹H NMR (400 MHz, C₆D₆): δ 0.387 (dd, *J*₁ = 6.6 Hz, *J*₂ = 2.1 Hz, 6H), 0.60 (multiplet, 2H), 0.904 (h, *J* = 6.7 Hz, 1H), 1.894 (br, 1H), 2.023 (br, 1H), 3.187 (br, 1H), 3.398 (br, 1H), 6.37–6.45 (multiplet, 2H), 6.48–6.64 (multiplet, 6H), 6.66–6.74 (multiplet, 2H), 6.78–6.92 (multiplet, 4H), 6.95–7.10 (multiplet, 4H), 7.13–7.28 (multiplet, 6H), 7.33–7.50 (multiplet, 5H), 7.599 (td, *J*₁ = 7.7 Hz, *J*₂ = 2.8 Hz, 2H), 7.742 (br, 2H), 7.94–8.14 (multiplet, 4H). ³¹P{¹H} (C₆D₆): δ 15.12 (d, *J*_{pp} = 39 Hz), 27.81 (d, *J*_{pp} = 35 Hz). ¹⁹F{¹H} (C₆D₆): -77.21 (s). IR (C₆H₆): 3310 w, 3216 w, 2924 w, 2857 w, 1576 m, 1437 m, 1284 s, 1259 m, 1224 m, 1099m, 816 w, 748 w. Anal. Calcd for C₅₆H₅₀F₃NO₃P₂PdS·1/2C₇H₈: C, 65.65; H, 5.00; N, 1.29. Found: C, 65.75; H, 4.94; N, 1.01.

Preparation of (BINAP)Pd(Ph)Cl. (BINAP)Pd(Ph)Br (250 mg, 0.28 mmol) was suspended in 10 mL of toluene. While stirring, *n*-octylamine (36.5 mg, 0.28 mmol) was added to the reaction mixture, followed by silver trifluoromethanesulfonate (76.1 mg, 0.30 mmol). A fine white precipitate formed immediately upon addition of AgOTf, and the color of the solution changed from pale yellow to almost colorless. After stirring at

room temperature for 5 min, the solution was carefully decanted and filtered through a plug of Celite. The precipitate was extracted with 2 mL of toluene, and the extract was added to the supernatant after filtration through a plug of Celite. The resulting solution was added dropwise to a solution of tetraoctylammonium chloride (142.0 mg, 0.284 mmol) in toluene with stirring. The resulting pale yellow solution was concentrated to 1/10th its original volume, layered with pentane, and placed in a freezer at -34 °C. A pale cream-colored solid was recovered (196.1 mg, 83% yield). ¹H NMR (400 MHz, CD₂Cl₂): δ 6.508 (broad, 2H), 6.58 (d, *J* = 8.8 Hz, 1H), 6.697 (multiplet, 3H), 6.75–6.82 (multiplet, 2H), 6.84–6.93 (multiplet, 3H), 6.94–7.10 (multiplet, 6H), 7.15–7.27 (multiplet, 3H), 7.29–7.47 (multiplet, 7H), 7.49–7.63 (multiplet, 6H), 7.72–7.84 (multiplet, 3H), 7.966 (dd, *J*₁ = 9.0 Hz, *J*₂ = 1.6 Hz, 1H). ³¹P{¹H} (C₆D₆): δ 13.69 (d, *J*_{pp} = 39 Hz), 30.54 (d, *J*_{pp} = 39 Hz). Anal. Calcd for C₅₀H₃₇P₂PdCl: C, 71.35; H, 4.43. Found: C, 71.02; H, 4.45.

Preparation of (BINAP)Pd(Ph)I. (BINAP)Pd(Ph)Br (250 mg, 0.28 mmol) was suspended in 10 mL of toluene. While stirring, *n*-octylamine (36.5 mg, 0.28 mmol) was added to the reaction mixture, followed by silver trifluoromethanesulfonate (76.1 mg, 0.30 mmol). A fine white precipitate formed immediately upon addition of AgOTf, and the color of the solution changed from pale yellow to almost colorless. After stirring at room temperature for 5 min, the solution was carefully decanted and filtered through a plug of Celite. The precipitate was extracted with 2 mL of toluene, and the extract was added to the supernatant after filtration through a plug of Celite. The resulting solution was added dropwise to a suspension of tetraheptylammonium iodide (166.9 mg, 0.31 mmol) in toluene with stirring. The resulting pale yellow suspension was concentrated to 1/10th its original volume, layered with pentane, and placed in a freezer at -34 °C. A pale yellow solid was recovered (105.1 mg, 39.9% yield). ¹H NMR (400 MHz, CD₂Cl₂): δ 6.478 (broad, 2H), 6.52 (d, *J* = 8.8 Hz, 1H), 6.72 (multiplet, 3H), 6.76–6.80 (multiplet, 2H), 6.82–6.89 (multiplet, 3H), 6.94–7.25 (multiplet, 9H), 7.33–7.48 (multiplet, 7H), 7.50–7.68 (multiplet, 6H), 7.74–7.90 (multiplet, 3H), 7.85 (dd, *J*₁ = 8.9 Hz, *J*₂ = 1.6 Hz, 1H). ³¹P{¹H} (C₆D₆): δ 9.29 (d, *J*_{pp} = 41 Hz), 21.20 (d, *J*_{pp} = 39 Hz). Anal. Calcd for C₅₀H₃₇P₂PdI: C, 64.36; H, 4.00. Found: C, 64.69; H, 4.00.

Thermolysis of [(BINAP)Pd(Ph)(H₂N(CH₂)₇CH₃)]OTf. [(BINAP)Pd(Ph)(H₂N(CH₂)₇CH₃)]OTf (10 mg, 9.2 μmol) was dissolved in 0.6 mL of toluene. The solution was transferred to a screw-capped NMR tube equipped with a PTFE-lined septum cap. An initial ³¹P{¹H} NMR spectrum was recorded, and the solution was heated at 60 °C in an oil bath. After 6 h of heating, no color change was observed, and ³¹P{¹H} NMR spectrometry showed that no change had occurred. The sample was then returned to an oil bath and heated at 80 °C. After 30 min of reaction time the color had changed to light orange. ³¹P{¹H} NMR spectroscopy showed that ca. 70% of the starting material had reacted. Further heating (6 h) showed complete conversion of **2a** and the formation of several unidentified ³¹P{¹H} resonances. DMPE (4.6 μL, 4.2 mg, 27.1 μmol) was then added to the sample, and a ³¹P{¹H} spectrum was recorded. A resonance due to Pd(DMPE)₂ was observed, but no resonances for free PPh₃ or free BINAP were observed. No *N*-octylaniline was detected by GC/MS analysis of the reaction solution.

Reaction of [(BINAP)Pd(Ph)(H₂N(CH₂)₇CH₃)]OTf with NaO-*t*-Bu. [(BINAP)Pd(Ph)(H₂N(CH₂)₇CH₃)]OTf (10 mg, 9.2 μmol) and 1,3,5-trimethoxybenzene (0.7 mg, 4.2 μmol) were dissolved in benzene-*d*₆. A ¹H NMR spectrum was recorded. NaO-*t*-Bu (1.8 mg, 18.7 μmol) was added to the tube, followed by BINAP (11.5 mg, 18.5 μmol). The tube was resealed and shaken. The immediate appearance of a dark red color, due to Pd(BINAP)₂, was observed. A ¹H NMR spectrum was recorded, and the yield of *N*-octylaniline was determined by

integrating the α -CH₂ resonances of the amine complex and *N*-octylaniline vs resonances of the internal standard.

Reaction of [(BINAP)Pd(Ph)(H₂N(CH₂)₇CH₃)]OTf with Cs₂CO₃ and K₃PO₄. [(BINAP)Pd(Ph)(H₂N(CH₂)₇CH₃)]OTf (25 mg, 23.1 μ mol), BINAP (28.7 mg, 46.1 μ mol), and 1,3,5-trimethoxybenzene (3.9 mg, 25.1 μ mol, internal standard) were dissolved in 4 mL of toluene-*d*₈. A ¹H NMR spectrum of this solution was recorded. Cs₂CO₃ (9.0 mg, 27.6 μ mol) or K₃PO₄ (6.0 mg, 36.6 μ mol) were weighed into two separate screw-capped vials. A 1.2 mL portion of the solution described above was transferred into each vial. A magnetic stir bar was added, and the vials were sealed with PTFE-lined septum screw-caps. The suspensions were allowed to stand at room temperature with vigorous stirring for 2 h. In both cases, only a very faint pink color developed due to the formation of small amounts of Pd(BINAP)₂. A ¹H NMR spectrum revealed that the conversion of the starting material was negligible. The vials were then removed from the glovebox and placed in an oil bath heated to 50 °C. After 7 h ¹H NMR spectra of both reactions were recorded, and after 18 h a ¹H NMR spectrum for the reaction with K₃PO₄ was recorded. The yields of *N*-octylaniline were determined by integrating the α -CH₂ resonances of the amine complex and products vs resonances of the internal standard. Complete conversion of the starting material for reaction with Cs₂CO₃ after 7 h and for reaction with K₃PO₄ after 18 h was confirmed by ³¹P{¹H} NMR spectroscopy.

Reaction of (BINAP)Pd(Ph)(Br) with *n*-Octylamine and Cs₂CO₃. (BINAP)Pd(Ph)(Br) (4.0 mg, 4.5 μ mol), BINAP (5.6 mg, 9.0 μ mol), and 1,3,5-trimethoxybenzene (1.0 mg, 6.4 μ mol, internal standard) were dissolved in 1 mL of benzene-*d*₆. A ¹H NMR spectrum of this solution was recorded. Cs₂CO₃ (9.0 mg, 27.6 μ mol) was weighed into a screw-capped vial and then added to the solution described above. A magnetic stir bar was added, and the vial was sealed with a PTFE-lined septum screw-cap. The suspension was allowed to stand at room temperature with vigorous stirring for 1 h. Only a very faint pink color developed due to the formation of small amounts of Pd(BINAP)₂. A ¹H NMR spectrum revealed that the conversion of the starting material was negligible. The vial was then removed from the glovebox and placed in an oil bath heated to 50 °C. After 1, 3, and 12 h ¹H NMR spectra were recorded. No *N*-octylaniline was detected. A ³¹P{¹H} NMR spectrum of the reaction mixture revealed that the (BINAP)-Pd(Ph)Br starting material had been completely consumed. GC/MS analysis of the reaction mixture revealed PPh₃ had been produced but showed no *N*-octylaniline.

Determination of Rate Constants for the Oxidative Addition of PhI, PhOTf, and PhBr to Pd(BINAP)₂. Separate stock solutions of Pd(BINAP)₂, BINAP, PhI, PhOTf, PhBr, and *n*-octylamine in benzene were prepared. Similar stock solutions were prepared in THF and 2,5-dimethyl-THF. The stock solutions were stored at -35 °C in a freezer. Samples were prepared by adding stock solutions into 5 mL volumetric flasks. Each flask was then filled to the 5 mL mark with the appropriate solvent. The resulting solutions were shaken and transferred (~3 mL) to quartz cuvettes that were fitted with airtight Teflon valves. The UV-visible spectrometer cell block was warmed to 40 °C for reactions of PhI and to 45 °C for reactions of PhOTf and PhBr. The absorbance of Pd(BINAP)₂ was monitored at $\lambda = 519$ nm over at least three half-lives, with a 1 s signal averaging time and 30 s between acquisitions. Kinetic data were fit to the expression $A_{519} = B e^{-kt} + c$, in which k is the pseudo-first-order rate constant k_{obs} . When obtaining k_{obs} for addition of PhI, experiments to determine the reaction order in BINAP contained a PhI concentration

that was fixed at 1.80×10^{-6} M, a Pd(BINAP)₂ concentration that was set to 8.55×10^{-7} M, and a concentration of BINAP that was varied from 1.70×10^{-4} to 1.08×10^{-3} M. For experiments to determine the reaction order in PhI, [Pd(BINAP)₂] was fixed at 4.27×10^{-7} , 8.55×10^{-7} , 2.26×10^{-5} , 1.35×10^{-6} , 5.62×10^{-6} , and 2.25×10^{-5} M. The concentration of BINAP was held constant at 1.70×10^{-4} M, and the concentration of PhI was varied from 8.94×10^{-7} to 4.20 M. For the determination of the effect of varying solvent and additives the concentrations of Pd(BINAP)₂, BINAP, and PhI were fixed at 8.55×10^{-7} , 1.70×10^{-4} , and 1.80×10^{-6} M, respectively. When obtaining k_{obs} values for the addition of PhOTf, experiments to determine the reaction order in BINAP contained a PhOTf concentration that was fixed at 2.26×10^{-4} M, a Pd(BINAP)₂ concentration that was fixed at 2.25×10^{-5} M, an *n*-octylamine concentration that was 1.13×10^{-4} M, and a concentration of BINAP that was varied from 170×10^{-4} to 6.78×10^{-4} M. For experiments to determine the reaction order in PhOTf, [Pd(BINAP)₂] was fixed at 2.25×10^{-5} M, the *n*-octylamine concentration was fixed at 1.13×10^{-4} M, [BINAP] was held constant at 1.70×10^{-4} M, and [PhOTf] was varied between 2.26×10^{-4} and 1.36 M. For the determination of solvent, amine, and additive effects the concentrations of Pd(BINAP)₂, BINAP, *n*-octylamine, and PhOTf were fixed at 2.25×10^{-5} , 1.70×10^{-4} , 1.13×10^{-4} , and 2.26×10^{-4} M, respectively. When obtaining k_{obs} values for addition of PhBr, experiments to determine the reaction order in PhBr contained [Pd(BINAP)₂] that was fixed at 2.25×10^{-5} M, [BINAP] that was held constant at 1.70×10^{-4} M, and [PhBr] that was varied between 0.50 and 4.00 M.

X-ray Crystal Structure of [(BINAP)Pd(Ph)(H₂N(CH₂)₂CH(CH₃)₂)]OTf (2b). A colorless plate crystal of C₅₆H₅₀N₃F₃P₂DdSPd·0.75(C₇H₁₆) was mounted on a glass fiber, and all measurements were made on a Nonius KappaCCD diffractometer with graphite-monochromated Mo K α radiation. The data were collected at a temperature of -90 ± 1 °C to a maximum 2θ value of 50.1°. Of the 9399 reflections that were collected, 5096 were unique ($R_{\text{int}} = 0.102$). The structure was solved by the Patterson method and expanded using Fourier techniques.¹⁴¹ The final cycle of full-matrix least-squares refinement¹⁴² was based on 2565 observed reflections ($I > 3.00\sigma(I)$) and 632 variable parameters and converged (largest parameter shift was 0.06 times its esd) with unweighted and weighted agreement factors of $R = 0.055$ and $R_w = 0.050$. For details on data acquisition and structure solution, see the Supporting Information.

Acknowledgment. We are grateful to the NIH (R01GM55382-02-04) for support of this work.

Supporting Information Available: Tables of positional parameters and B_{eq} , U values, intramolecular distances, intramolecular bond angles, and torsion or conformational angles for hydrogen and non-hydrogen atoms for **2b** (PDF). This material is available free of charge via the Internet at <http://pubs.acs.org>.

OM0108088

(141) Beurskens, P. T., Admiraal, G., Beurskens, G., Bosman, W. P., de Gelder, R., Israel, R., Smits, J. M. M. *DIRDIF94*. The DIRDIF-94 program System; Technical Report of the Crystallography Laboratory; University of Nijmegen: The Netherlands, 1994.

(142) Least-squares function minimized: $\sum w(|F_o| - |F_c|)^2$, where $w = 4F_o^2/\sigma^2(F_o^2) = [\sigma^2(F_o) + (pF_o/2)^2]^{-1}$, $F_o^2 = \sum(C - RB)/Lp$, and $\sigma^2(F_o^2) = [\sum^2(C + R^2B) + (pF_o^2)^2]/Lp^2$, S = scan rate, C = total integrated peak count, R = ratio of scan time to background counting time, B = total background count, Lp = Lorentz-polarization factor, p = p-factor.